PHYSICAL REVIEW B **82**, 195412 (2010)

Observation of excitonic effects in metallic single-walled carbon nanotubes

Patrick May,[1,*] Hagen Telg,[1] Guofang Zhong,[2] John Robertson,[2] Christian Thomsen,[1] and Janina Maultzsch[1]
[1]*Institut für Festkörperphysik, Technische Universität Berlin, Hardenbergstr. 36, D-10623 Berlin, Germany*
[2]*Department of Engineering, University of Cambridge, Cambridge CB3 0FA, United Kingdom*
(Received 2 July 2010; revised manuscript received 14 October 2010; published 8 November 2010)

Excitonic effects of metallic single-walled carbon nanotubes are measured with temperature-dependent resonant Raman spectroscopy. By changing the temperature in the range of 300–870 K, we observe variations in the optical transition energy E_{ii} as well as in the maximum Raman intensity. We find both dependences to be different for semiconducting and metallic single-walled carbon nanotubes. We suggest an interpretation in terms of excitons dissociated into free electron-hole pairs at temperatures related to the exciton binding energy. We furthermore discuss how the oscillator strength is influenced by temperature.

DOI: 10.1103/PhysRevB.82.195412 PACS number(s): 78.67.Ch

Single-walled carbon nanotubes (SWCNTs) can be described as rolled up strips of graphene, and therefore belong to the class of quasi-one-dimensional systems. They are promising candidates for a variety of optoelectronic applications, such as nanoscale field effect transistors, electrically excited single-molecule light sources and nanosensors.[1–3] Optical transitions play a central role in understanding the fundamental properties of carbon nanotubes.[4] Both theoretical and experimental studies revealed that light absorption excites strongly correlated electron-hole pairs in semiconducting nanotubes. These excitons have binding energies of several hundred millielectron volts, owing to their enhanced Coulomb interaction.[5–8] Screening of electrons is rather effective in metals, which prevents the formation of excitons. Therefore it has been a longstanding question to what extend optical transitions are dominated by excitons in metallic SWCNTs. Theoretical calculations predict the existence with binding energies around 50–100 meV for the first optical transition E_{11}^M.[9–11] Absorption measurements on a large diameter individual metallic nanotube showed evidence for considerable strength of electron-hole interaction in metallic nanotubes.[12] However, it is experimentally challenging to determine the exciton binding energy of SWCNTs. Theory predicts a variety of excitonic states with different symmetry. One-photon spectroscopy couples to optically active excitonic states with odd (u) symmetry with respect to rotations about the U axis.[13] The lowest lying dark state is dipole forbidden by symmetry.[14] The technique of two-photon photoluminescence (PL) spectroscopy, which was applied to obtain binding energies of semiconducting nanotubes, cannot be extended to metallic tubes due to quenching of radiative decay.[5,6] Another technique to measure the exciton binding energy is to perform temperature-dependent measurements of the particular optical transition. The temperature-induced dissociation of the excitons results in an increase in the transition energy when the thermal energy matches the binding energy of the excitons.[15] In order to apply this technique to semiconducting nanotubes, temperatures on the order of at least 3000 K would be necessary, which is beyond the thermal stability of nanotubes. However, assuming an exciton binding energy of $\approx$50 meV in metallic nanotubes this technique appears to be promising regarding the experimental observation of the exciton binding energy in metallic nanotubes.

In this work, we present a temperature-dependent resonant Raman study on the optical transition energies in metallic and semiconducting carbon nanotubes. We varied the temperature between $\approx$300 and 870 K and collected resonance profiles for each temperature of the radial breathing mode (RBM) from different semiconducting and metallic nanotubes. For semiconducting nanotubes we observe a monotonic decrease in the transition energy with increasing temperature. In metallic nanotubes we first observe a decrease similar to that of the semiconducting tube, however for temperatures above 570 K, the transition energy E_{ii} starts to increase again. We attribute this behavior in metallic nanotubes to dissociation of excitons into free electron-hole pairs at temperatures related to the exciton binding energy. We estimate a binding energy of around 50 meV.

The measurements were performed on vertically aligned single-walled carbon nanotubes. They were grown by chemical vapor deposition resulting in a diameter distribution between 0.5 and 2 nm.[16,17] The excitation by dye lasers was carried out between 1.8 and 2.25 eV, therefore accessing the first transition E_{11}^M of metallic nanotubes and the second transition E_{22}^S of semiconducting nanotubes. In order to rule out temperature-induced effects by the laser, the power was kept around $\approx$500 μW,[18] while the spot size was 2 μm. The temperature of the sample, which was in an argon gas environment, was controlled by a Linkham (THMS600) heating stage in the range of 298–873 K. The scattered light was collected in backscattering geometry and dispersed by a Dilor XY800 triple monochromator equipped with a nitrogen cooled charge-coupled device. The Raman intensities were normalized with respect to the integration time and laser power. Furthermore we took the system response into account by normalizing the Raman intensities to the nonresonant Raman signal of CaF_2.[19]

In Fig. 1 we show the Raman spectra excited at 2.07 eV for three different temperatures. The upper temperature limit was 770 K for the semiconducting tube. At higher temperatures, the intensity was too weak to resolve the RBM peaks separately. We observe several RBMs around 210 and 250 cm^{-1}. A first rough assignment can be made by considering the excitation energy. Thus, the first group of peaks can be assigned to metallic nanotubes and the latter to semiconducting ones.[20] Overall, the absolute RBM intensity de-

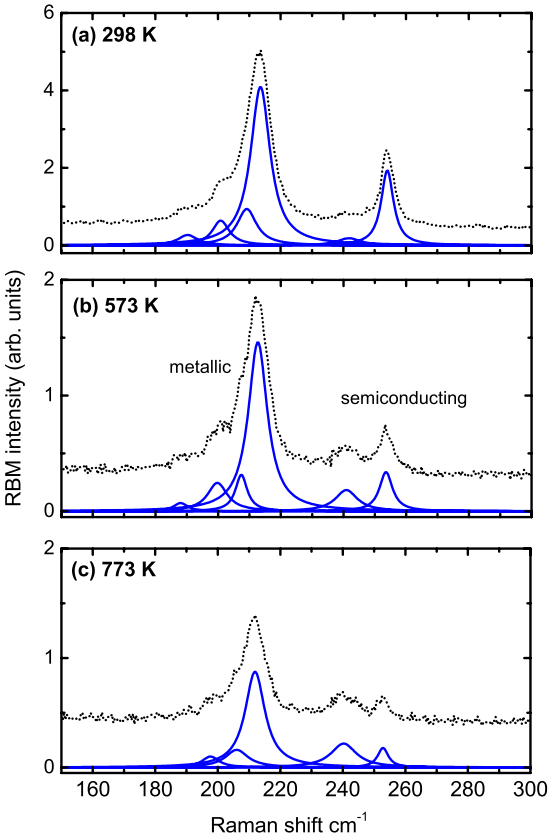

FIG. 1. (Color online) RBM spectra of single-walled carbon nanotubes for different temperatures excited at 2.07 eV. Solid lines indicate Lorentzian fits to the experimental data. The RBM intensity [intensity units between (a), (b), and (c) can be compared] decreases as the temperature increases.

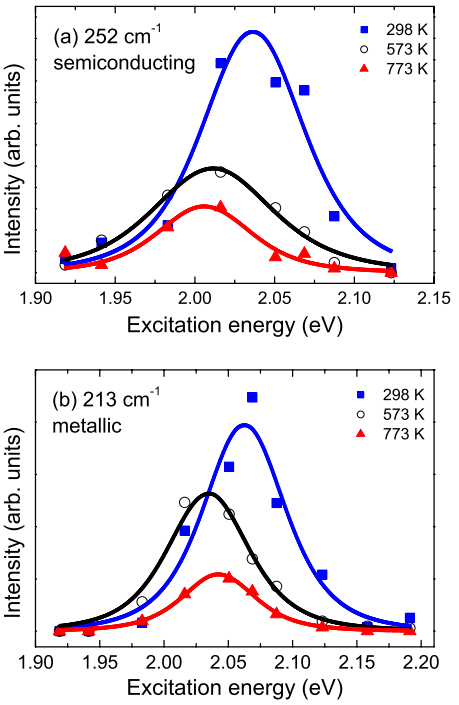

FIG. 2. (Color online) Raman resonance profiles of the radial breathing mode (a) of a semiconducting nanotube and (b) for the metallic nanotube at different temperatures. Solid lines indicate theoretical fits to the experimental data, which are represented by symbols.

creases with increasing temperature. However, the relative intensities of different peaks change as can be seen at around 240 cm^{-1}, where the relative peak intensity increases in comparison to peaks at around 210 cm^{-1}. This variation is due to a change in the optical transition energy E_{ii} with temperature. In the analysis discussed below we examine this behavior by studying resonant Raman profiles. We put the focus on one RBM of each nanotube species, each with the strongest Raman signal, the metallic tube at 213 cm^{-1} and the semiconducting tube at 252 cm^{-1}. Following the systematics described in Ref. 20, we assign the RBM at 252 cm^{-1} to the semiconducting (11,1) tube excited into the second optical transition E_{22}^{S}. The (11,1) tube belongs to the $\nu=+1$ family with $\nu=(n-m)$ mod3. The RBM at 213 cm^{-1} can be assigned to the metallic (13,1) tube excited into the first optical transition E_{11}^{M}.

Figure 2(a) shows the resonance profile of the semiconducting (11,1) tube for three different temperatures. As we would expect for a classical semiconductor, we observe a shift of the resonance profile, thus the transition energy, to lower energies as the temperature increases.[21–23] Figure 2(b) shows the resonance profiles of the metallic (13,1) nanotube for the same temperatures. Apparently we do not observe a monotonic shift as for the semiconducting nanotube. In order to study this difference between the temperature dependence of the transition energies in semiconducting and metallic nanotubes, we collected resonance profiles from the (11,1) and the (13,1) nanotube at various temperatures. The transition energies are then obtained by fitting the resonance profiles with[24]

$$I(E_l) = \left(\frac{\mathcal{M}c}{\hbar\omega_{\mathrm{RBM}}}\right)^2 \left| \frac{1}{(E_l - E_{ii} - i\Gamma/2)} - \frac{1}{(E_l - \hbar\omega_{\mathrm{RBM}} - E_{ii} - i\Gamma/2)} \right|^2, \quad (1)$$

where $\mathcal{M}$ contains all matrix elements and c summarizes all remaining factors. E_l is the laser energy, E_{ii} the energy of the allowed optical transition, and Γ the broadening of the intermediate electronic state. The first and second term represents ingoing and outgoing resonance, respectively. We estimated a constant error of ± 5 meV in determining E_{ii}.

The resulting transition energy as a function of temperature of both the semiconducting and the metallic nanotube is shown in Fig. 3. While the semiconducting tube shows a monotonic downshift across the entire temperature range, the metallic tube shows a sudden upshift of the transition energy above $\approx$570 K. Below this temperature we also observe a monotonic downshift of E_{ii} for the metallic nanotube.

First we discuss the monotonic decrease in the transition energy with temperature in semiconducting nanotubes and in metallic nanotubes up to $\approx$570 K. Tentatively we perform a linear fit to the data, which yields a redshift of -6.38×10^{-5} eV K^{-1} for the semiconducting tube. The downshift of the transition energy can be explained by the temperature

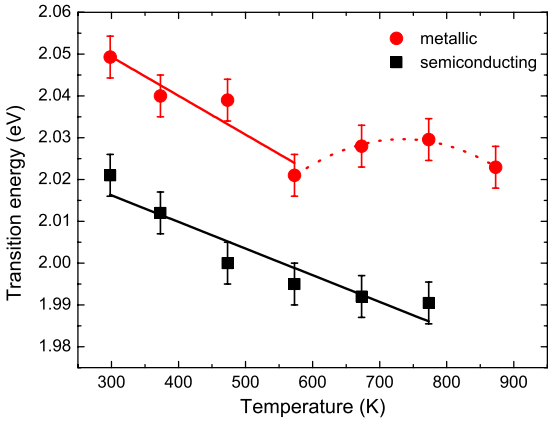

FIG. 3. (Color online) Experimental transition energies E_{ii} as a function of temperature for the metallic and semiconducting nanotubes. The lines are linear fits to the data. The dotted line is a guide to the eyes.

dependence of optical transitions and the softening of the band gap at higher temperatures due to lattice expansion and electron-phonon coupling.[21,25] Downshifts of E_{ii} in carbon nanotubes based on the electron-phonon coupling model were presented in Refs. 10 and 21. In these calculations, however, excitonic effects and the characteristics of temperatures above 600 K were not shown. Table I shows a comparison of our results with other experimental and theoretical data. For the semiconducting tube, we find reasonable agreement with the predicted shift of approximately -4.4×10^{-5} eV K^{-1} for the E_{11} transition in the (11,1) tube[21] and with experimental data of Cronin *et al.*[25] In Ref. 25 the experimental data were not assigned to a particular (n,m) tube. The calculated shifts in Ref. 25 for the metallic nanotubes are in the range of -6.0 to -8.8×10^{-5} eV K^{-1}. Our result of -9.30×10^{-5} eV K^{-1} up to 570 K is in reasonable agreement. We can attribute our slightly different values to the analysis of different chiral indices.

Let us now have a closer look at the increase in transition energy of the metallic nanotube above ≈570 K. We explain this behavior in terms of excitons which are dissociated into free electron-hole pairs at temperatures related to the exciton binding energy.[15] When the excitons dissociate, we no longer observe the excitonic transition but that of the free particles. After all excitons are dissociated, the optical transition again shifts down in energy due to electron-phonon coupling. The reason why we do not observe an upshift for the semiconducting tube is that the thermal energy is not sufficient to break excitons, which have binding energies of several hundred millielectron volts.[5,6] There are two possibilities to derive the exciton binding energy from the temperature-dependent shift of the transition energy. The first is the starting point of the blueshift at 570 K. This temperature corresponds to an energy of around 50 meV, which is in agreement with theoretically predicted values of the binding energies in metallic nanotubes.[9–11]

The value of 50 meV was also deduced from absorption measurements into the second optical transition E_{22} of an individual (21,21) nanotube.[12] However, this nanotube had approximately twice the diameter compared to the tube in our experiment. Since the exciton binding energy is predicted to be diameter dependent,[8,14,27] we would expect even higher binding energies in our experiment. On the other hand, the development of the exciton binding energy in higher optical transitions is still under discussion. References 11 and 28 suggest increasing binding energy in higher optical transitions, while Refs. 29 and 30 showed different exciton behavior for E_{33} and E_{44} than for E_{11} and E_{22}. Therefore, the dependence of the exciton binding energy on the transition might partly compensate the diameter dependence of the exciton binding energy.

The other possibility to estimate the exciton binding energy from our data is the difference between the initial linear fit (red dashed line) of the metallic transition energy and the

TABLE I. Temperature dependence of the transition energy from experiments and theory. We assumed the shifts to be linear for the temperature region above 298 K, disregarding the nonlinear behavior at low temperatures for our comparison with other results.

Tube	Range (K)	Shift (eV K^{-1})	Method
	This work		
(11,1)	298–773	-6.38×10^{-5}	Raman
(13,1)	298–573	-9.30×10^{-5}	Raman
	Ref. 21		
(11,1)	0–600	-4.4×10^{-5}	Calc.[a]
	Ref. 25[b]		
$\nu=-1$	300–573	-11.7×10^{-5}	Raman
$\nu=-1$	300–573	-4.1×10^{-5}	Raman
179 cm^{-1} (met.)[c]	300–573	-7.1×10^{-5}	Raman
160 cm^{-1} (met.)[c]	300–573	-2.5×10^{-5}	Raman
(10,0)	300–573	-9.2×10^{-5}	Ext. TB[d]
(10,2)	300–573	-7.5×10^{-5}	Ext. TB[d]
(11,0)	300–573	-7.3×10^{-5}	Ext. TB[d]
(13,0)	300–573	-6.1×10^{-5}	Ext. TB[d]
(11,0)	300–573	-7.3×10^{-5}	Ext. TB[d]
Met. E_{11}^{-} [e] (18,0)	300–573	-8.8×10^{-5}	Ext. TB[d]
Met. E_{11}^{+} [e] (18,0)	300–573	-6.0×10^{-5}	Ext. TB[d]
	Ref. 26[f]		
(7,6)	5–300	-5.0×10^{-5}	PL[g]
(9,8)	5–300	$\approx-1.1\times10^{-5}$	PL
(12,2)	5–300	-3.0×10^{-5}	PL

[a]Frozen-phonon calculation of electron-phonon coupling for E_{11}^{S}.
[b]Experimental data were measured on individual suspended nanotubes.
[c]The RBMs were not assigned to a specific nanotube but to one out of (18,0), (19,1), (12,12), or (14,8) (Ref. 25).
[d]Extended tight-binding calculation.
[e]Corresponds to the splitting of the first transition in metallic tubes.
[f](7,6) and (9,8) are individual tubes; (12,2) is from a pillar suspended ensemble.
[g]Experimental photoluminescence data of E_{11}^{S}.

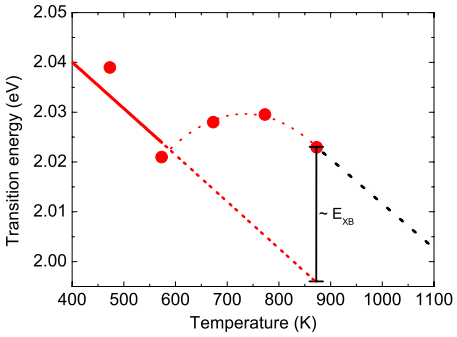

FIG. 4. (Color online) Extrapolation of the linear fit to the transition energies of the metallic tube from Fig. 3 (lower red dashed line) and estimation of the upshift of this line above 850 K. The vertical bar indicates the estimation for the exciton binding energy E_{XB}.

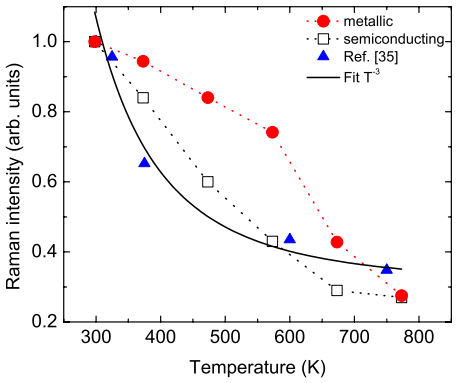

FIG. 5. (Color online) Maximum of the resonance profile (i.e., the areal intensity of the RBM peak in full resonance) as function of temperature for semiconducting (black squares) and metallic (red dots) nanotubes. The semiconducting data are fitted with $f^2 \propto T^{-3}$ and compared with results of Ref. 32 (blue triangels). The values of the intensity are normalized to the intensity at 300 K for better graphical representation. Dashed lines are guide to the eyes.

downshift at temperatures above 850 K (black dashed line), which is shown in Fig. 4. Without dissociation of excitons, we would expect a further linear downshift (red dashed line) at temperatures above 570 K. The difference between this line and the experimental data is therefore another measure for the exciton binding energy of the metallic nanotube. From Fig. 4 we thus estimate a binding energy of approximately 27 meV. However, it is not known whether the temperature shift of the band gap (noninteracting electron-hole pairs) and of the excitonic energies is the same.

In order to examine how thermal expansion contributes to the shifts, we discuss two scenarios. First, we consider the case of nonisotropic expansion of the nanotube, following Eq. (2) of Ref. 25 for the shift ΔE_{ii} in transition energy:

$$\Delta E_{ii} = -2E_{ii}\epsilon_r - 3\gamma_0(-1)^i(-1)^\nu(\epsilon_r - \epsilon_z)\cos(3\Theta), \quad (2)$$

where ϵ_r and ϵ_z are the radial and axial strain, Θ is the chiral angle, γ_0 (2.9 eV) is the next-nearest-neighbor hopping matrix element of the tight-binding (TB) model and ν is +1 for both the metallic and semiconducting nanotubes in our case. If we insert for radial and axial expansion the values given in Ref. 31 for the metallic (10,10) nanotube we obtain a transition energy shift of 1.5×10^{-5} eV K^{-1}. This is approximately six times less than our shift and of opposite direction. Second, we can assume isotropic thermal expansion for the metallic tube with a (negative) thermal-expansion coefficient similar to graphite, -1.0×10^{-6} K^{-1}. This would also result in an upshift of transition energy with increasing temperature, and the value of $\approx 4 \times 10^{-6}$ eV K^{-1} is one order of magnitude smaller than what we measured. Indeed, the thermal expansion coefficient of graphite changes sign in approximately the same temperature range as the sign change observed in the E_{11}^M shift. However, the sign of the E_{11}^M shift observed in our experiment is opposite to what would be expected from the graphite thermal expansion. Therefore, we assume the effect of thermal expansion is negligible for the interpretation of our experimental results. A similar conclusion was obtained in Ref. 21 for the band gap of semiconducting tubes.

Further evidence for the dissociation of excitons in metallic nanotubes can be found in the temperature-dependent Raman intensity, which is proportional to the square of the oscillator strength of the corresponding optical transition. In Fig. 5 we plot the RBM intensity at the maximum of the resonance profile of the semiconducting and the metallic nanotubes. In principle, one should also take into account the width of the resonance profiles, however, we did not observe a systematic dependence of the broadening parameter Γ on temperature, as the values scatter widely. The values range from 85 to 110 meV for the metallic and from 90 to 140 meV for the semiconducting nanotube.

For both the metallic and the semiconducting nanotubes we observe a decrease in the maximum intensity with increasing temperature. A general decrease can be explained by an increase in the lifetime broadening of the excitonic states.[33] The broadening, in turn, leads to a decrease in the maximum Raman intensity in the resonant Raman process.[34] This however does not explain the rapid decrease in the maximum intensity of the metallic (13,1) tube, which we observe between 570 and 670 K. Comparing the absolute values between 570 and 770 K, the intensity of the metallic tube decreases by a factor of 2.9 while the one of the semiconducting decreases only by a factor of 1.6. It has been predicted that excitonic transitions in carbon nanotubes are in general stronger than band-to-band transitions,[35] i.e., excitonic effects enhance the optical matrix elements and thus the resonance Raman intensity. Therefore the rapid decrease in the Raman intensity of the metallic tube can be explained by dissociation of excitons at ≈ 50 meV.

To treat the behavior of the oscillator strength theoretically, we consider the following. The experimentally observed exciton oscillator strength is inversely proportional to the effective decay rate w_{eff} or directly proportional to the lifetime τ_{eff}. At low temperatures, the effective radiative lifetime in semiconducting carbon nanotubes has a square-root temperature dependence.[36,37] At higher temperatures (above ≈ 60 K), Perebeinos *et al.*[33] showed that the temperature dependence of the decay rate can be approximated by $w_{\mathrm{eff}} \propto T^{3/2}$. As the Raman intensity is proportional to the square of the oscillator strength (f), we expect it to depend as T^{-3} on temperature.

In Fig. 5 we show a fit of $f^2 \propto T^{-3}$ to the RBM maximum intensity of the semiconducting tube. We find reasonable agreement although our data are less steep than the $f^2 \propto T^{-3}$ fit. This might be due to symmetry breaking resulting in scattering between optically allowed and forbidden exciton states.[33] In this case the temperature dependence of f deviates from the T^{-3} behavior.[33] Moreover, the calculations in Ref. 33 were done for the lower transition E_{11}^S of semiconducting nanotubes, whereas our measurements are for the second transition E_{22}^S. Due to additional decay channels,[38] the temperature dependence of the oscillator strength is expected to be different in E_{22}^S from that in E_{11}^S. We further compare our areal intensity of the RBM peak in full resonance with recent data on electrically induced heating of an individual tube (triangles in Fig. 5).[32] These data agree quite well with the T^{-3} fit. Possible reasons for differences between our data and the data of Ref. 32 can be due to different conditions concerning the optical transition (E_{22}^S vs E_{33}^S) and environmentally vs electrically induced heating. Furthermore interactions among the tubes might change the oscillator strength. However, the RBM of Ref. 32 showed similar E_{ii} shift rates as our semiconducting nanotube.

For metallic tubes, to the best of our knowledge, no temperature-dependent calculations of the oscillator strength in E_{11}^M have been reported so far. It has been shown in Ref. 12 that due to their reduced exciton binding energies, metallic tubes exhibit a contribution of continuum transitions in their absorption spectra. The oscillator strength is thus distributed over both the excitonic and the continuum transition. Our results imply that at temperatures above 570 K the oscillator strength is fully restored in the continuum transition.

In summary, we observe different temperature dependences of the transition energies in semiconducting and metallic nanotubes. While the semiconducting nanotube shows a monotonic decrease, which is in good agreement with theory and previous experiments, the metallic nanotube shows a blueshift above 570 K. We interpret this in terms of excitons, which are dissociated by thermal energy. Hence, we derive an exciton binding energy on the order of 50 meV for the metallic (13,1) tube. Our interpretation is further supported by the observation of a stronger temperature-induced decrease in the Raman scattering efficiency in case of the metallic nanotube compared to the semiconducting tube.

We acknowledge support from the DFG under Grant No. MA 4079/3-1. H.T. and G.Z. acknowledge funding from the European Union (Technotubes; Grant No. CP-IP 228579-1).

*pmay@physik.tu-berlin.de

[1] S. J. Tans, A. R. M. Verschueren, and C. Dekker, Nature (London) **393**, 49 (1998).
[2] J. A. Misewich, R. Martel, J. C. Tsang, S. Heinze, and J. Tersoff, Science **300**, 783 (2003).
[3] E. S. Snow, F. K. Perkins, E. J. Houser, S. C. Badescu, and T. L. Reinecke, Science **307**, 1942 (2005).
[4] S. Reich, C. Thomsen, and J. Maultzsch, *Carbon Nanotubes: Basic Concepts and Physical Properties* (Wiley-VCH, Berlin, 2004).
[5] J. Maultzsch, R. Pomraenke, S. Reich, E. Chang, D. Prezzi, A. Ruini, E. Molinari, M. S. Strano, C. Thomsen, and C. Lienau, Phys. Rev. B **72**, 241402(R) (2005).
[6] F. Wang, G. Dukovic, L. E. Brus, and T. F. Heinz, Science **308**, 838 (2005).
[7] E. Chang, G. Bussi, A. Ruini, and E. Molinari, Phys. Rev. Lett. **92**, 196401 (2004).
[8] V. Perebeinos, J. Tersoff, and P. Avouris, Phys. Rev. Lett. **92**, 257402 (2004).
[9] C. D. Spataru, S. Ismail-Beigi, L. X. Benedict, and S. G. Louie, Phys. Rev. Lett. **92**, 077402 (2004).
[10] J. Deslippe, C. Spataru, D. Prendergast, and S. G. Louie, Nano Lett. **7**, 1626 (2007).
[11] E. Malic, J. Maultzsch, S. Reich, and A. Knorr, Phys. Rev. B **82**, 035433 (2010).
[12] F. Wang, D. J. Cho, B. Kessler, J. Deslippe, P. J. Schuck, S. G. Louie, A. Zettl, T. F. Heinz, and Y. R. Shen, Phys. Rev. Lett. **99**, 227401 (2007).
[13] M. Damnjanović, I. Milošević, T. Vuković, and R. Sredanović, Phys. Rev. B **60**, 2728 (1999).
[14] H. Zhao and S. Mazumdar, Phys. Rev. Lett. **93**, 157402 (2004).
[15] M. Hugues, B. Damilano, J. Y. Duboz, and J. Massies, Phys. Rev. B **75**, 115337 (2007).
[16] J. Robertson, G. Zhong, H. Telg, C. Thomsen, J. H. Warner, G. A. D. Briggs, U. Dettlaf-Weglikowska, and S. Roth, Appl. Phys. Lett. **93**, 163111 (2008).
[17] G. Zhong, S. Hofmann, F. Yan, H. Telg, J. H. Warner, D. Eder, C. Thomsen, W. I. Milne, and J. Robertson, J. Phys. Chem. C **113**, 17321 (2009).
[18] F. Simon, R. Pfeiffer, and H. Kuzmany, Phys. Rev. B **74**, 121411 (2006).
[19] M. Grimsditch, M. Cardona, J. Calleja, and F. Meseguer, J. Raman Spectrosc. **10**, 77 (1981).
[20] J. Maultzsch, H. Telg, S. Reich, and C. Thomsen, Phys. Rev. B **72**, 205438 (2005).
[21] R. B. Capaz, C. D. Spataru, P. Tangney, M. L. Cohen, and S. G. Louie, Phys. Rev. Lett. **94**, 036801 (2005).
[22] M. Cardona, T. A. Meyer, and M. L. W. Thewalt, Phys. Rev. Lett. **92**, 196403 (2004).
[23] O. Madelung, *Semiconductors: Group IV Elements and III-V Compounds* (Springer, Berlin, 1991).
[24] M. Cardona, *Light Scattering in Solids II*, Topics in Applied Physics Vol. 50 (Springer, Berlin, 1982), p. 19.
[25] S. B. Cronin *et al.*, Phys. Rev. Lett. **96**, 127403 (2006).
[26] J. Lefebvre, P. Finnie, and Y. Homma, Phys. Rev. B **70**, 045419 (2004).
[27] C. L. Kane and E. J. Mele, Phys. Rev. Lett. **93**, 197402 (2004).
[28] K. Sato, R. Saito, J. Jiang, G. Dresselhaus, and M. S. Dresselhaus, Phys. Rev. B **76**, 195446 (2007).
[29] P. T. Araujo, S. K. Doorn, S. Kilina, S. Tretiak, E. Einarsson, S. Maruyama, H. Chacham, M. A. Pimenta, and A. Jorio, Phys. Rev. Lett. **98**, 067401 (2007).

[30] S. K. Doorn, P. T. Araujo, K. Hata, and A. Jorio, Phys. Rev. B **78**, 165408 (2008).
[31] P. K. Schelling and P. Keblinski, Phys. Rev. B **68**, 035425 (2003).
[32] M. Steiner, M. Freitag, V. Perebeinos, J. Tsang, J. Small, M. Kinoshita, D. Yuan, J. Liu, and P. Avouris, Nat. Nanotechnol. **4**, 320 (2009).
[33] V. Perebeinos, J. Tersoff, and P. Avouris, Nano Lett. **5**, 2495 (2005).
[34] H. Telg, J. Maultzsch, S. Reich, and C. Thomsen, Phys. Status Solidi B **244**, 4006 (2007).
[35] J. Jiang, R. Saito, K. Sato, J. S. Park, G. G. Samsonidze, A. Jorio, G. Dresselhaus, and M. S. Dresselhaus, Phys. Rev. B **75**, 035405 (2007).
[36] C. Spataru, S. Ismail-Beigi, R. Capaz, and S. Louie, Phys. Rev. Lett. **95**, 247402 (2005).
[37] F. Wang, G. Dukovic, L. Brus, and T. Heinz, Phys. Rev. Lett. **92**, 177401 (2004).
[38] S. Reich, C. Thomsen, and J. Robertson, Phys. Rev. Lett. **95**, 077402 (2005).